Frontiers of Physics
https://doi.org/10.1007/s11467-019-0919-y
Front. Phys.
14(6), 63603 (2019)

RESEARCH ARTICLE

Universal conductance fluctuations in Sierpinski carpets

Yu-Lei Han, Zhen-Hua Qiao†

ICQD, Hefei National Laboratory for Physical Sciences at Microscale, Synergetic Innovation Center of Quantum Information and Quantum Physics, CAS Key Laboratory of Strongly-Coupled Quantum Matter Physics, and Department of Physics, University of Science and Technology of China, Hefei 230026, China
Corresponding author. E-mail: †qiao@ustc.edu.cn
Received May 21, 2019; accepted June 18, 2019

We theoretically investigate the conductance fluctuation of two-terminal device in Sierpinski carpets. We find that, for the circular orthogonal ensemble (COE), the conductance fluctuation does not display a universal feature; but for circular unitary ensemble (CUE) without time-reversal symmetry or circular symplectic ensemble (CSE) without spin-rotational symmetry, the conductance fluctuation can reach an identical universal value of $0.74 \pm 0.01(e^2/h)$. We further find that the conductance distributions around the critical disorder strength for both CUE and CSE systems share the similar distribution forms. Our findings provide a better understanding of the electronic transport properties of the regular fractal structure.

Keywords electronic transport, conductance fluctuation

1 Introduction

Universal conductance fluctuation (UCF) is one of the striking features in mesoscopic electronic transport [1–3]. It is a quantum interference effect that occurs in systems with sample size being less than the phase coherence length. And the UCF amplitude only depends on the dimensionality and system symmetries [4–6]. According to random matrix theory [7], there are usually three ensembles due to different symmetries: (i) Circular orthogonal ensemble (COE), where both time-reversal and spin-rotation symmetries are preserved; (ii) Circular unitary ensemble (CUE), where the time-reversal symmetry is broken but the spin-rotation symmetry ia preserved; (iii) Circular symplectic ensemble (CSE), where the time-reversal symmetry is preserved but the spin-rotational symmetry is broken. These three ensembles can be indexed by $\beta = 1, 2, 4$, corresponding respectively to COE, CUE and CSE. For quantum dot, quasi-one dimensional, and two dimensional systems, the UCF at the diffusive regimes are respectively $\mathrm{rms}(G) = c_d/\sqrt{\beta}(e^2/h)$, where $c_d = 0.70, 0.73, 0.86$ [4–7].

So far, there have been tremendous focus on the UCF for the integer dimensions [8–22]. However, there is very limited study on the UCF in fractal dimension [23], which is also named as Hausdorff dimension measuring the dimensionality of self-similar structures [24]. As the simplest models of regular fractal structure, Sierpinski gasket and carpet have attracted numerous attentions. The related research mainly focused on the electronic transport properties [25–34], and the topological properties in Sierpinski lattices [35]. For example, Schwalm *et al.* investigated the conductance distribution in the presence of random bond disorder via length scaling theory and described the curves by two parameters that are independent of the model system [29]; spin-related transport study of fractal conductors proposed a spin filter based on Sierpinski carpet [32, 33]; and the nonzero Chern number in Sierpinski carpet under external magnetic field [35] demonstrates the extraordinary electronic properties in fractal dimension. In addition to the previous theoretical proposals, the realistic experimental realization of Sierpinski triangle fractals either by molecular self-assembling or by atomic manipulation [36, 37] arises some interesting questions: Does there exist a UCF in fractal dimension? How does the symmetry affect the conductance fluctuation?

Fractals are self-similarity patterns and can be iterated infinitely. According to the characteristics of fractal, it can be classified into different types, e.g., exact/quasi/statistical/qualitative self-similar patterns. As a representative exact self-similar fractal, we choose Sierpinski carpet to address the above questions. We provide a systematic investigation on the electronic transport properties of Sierpinski carpets in the presence of disorders. Unlike integral dimensions, we find that the Sierpinski carpets do not have a UCF at the COE situation; when the time-reversal symmetry or the spin-rotational symmetry is broken, we show that UCF can be reached at the CUE or CSE system, i.e., $\mathrm{rms}(G)$=$0.74\pm0.01(e^2/h)$; and the corresponding conductance distributions in the diffusive region for both CUE and CSE systems obey nearly the same distribution, i.e., normal distribution at the small conductance region but log-normal distribution at the large conductance region.

© Higher Education Press and Springer-Verlag GmbH Germany, part of Springer Nature 2019

2 Model system

In our numerical calculations, the tight-binding model Hamiltonian of square lattice system can be expressed as [38]:

$$H = -t \sum_{\langle ij\rangle,\alpha} c_{i\alpha}^{\dagger} c_{j\alpha} \mathrm{e}^{-\mathrm{i}2\pi\phi_{ij}} + \sum_{i\in B,\alpha} \epsilon_0 c_{i\alpha}^{\dagger} c_{i\alpha} + \mathrm{i}t_{\mathrm{SO}} \sum_{\langle ij\rangle,\alpha\gamma} \hat{\mathbf{e}}_z \cdot (\boldsymbol{\sigma}_{\boldsymbol{\alpha\gamma}} \times \boldsymbol{d}_{ij}) c_{i\alpha}^{\dagger} c_{j\gamma} + \sum_{i,\alpha} \epsilon_i c_{i\alpha}^{\dagger} c_{i\alpha},$$

where $c_{i\alpha}^{\dagger}$ ($c_{i\alpha}$) is the electron creation (annihilation) operator with spin α at site i, and t is the hopping energy between nearest neighbor sites. The effect of external magnetic field is considered by a Peierls phase factor $\phi_{ij} = \int \boldsymbol{A} \cdot \mathrm{d}l/\phi_0$ in the first term, where $\boldsymbol{A} = (-By, 0, 0)$ is vector potential with Landau gauge and $\phi_0 = h/e$ is the quantum of flux. The second term describes the removed region of Sierpinski carpet with a large on-site potential $\epsilon_0 = 10^7 t$, which has been elaborately tested for the convergence of conductance. The third term represents Rashba spin–orbit coupling with coupling strength t_{SO}, $\boldsymbol{\sigma}$ are the Pauli matrices and $\boldsymbol{d}_{ij}$ stands for the unit vector pointing from site j to site i. The last term corresponds to the Anderson type disorder with ϵ_i being uniformly distributed within the range of $[-W/2, W/2]$, where W characterizes the disorder strength.

In our consideration, the two-terminal electronic transport was evaluated by employing the Landauer–Büttiker formula [39] to calculate the conductance G, i.e., $G = (2e^2/h)\mathrm{Tr}(\Gamma_L G^r \Gamma_R G^a)$. Here $G^{r,a}$ are the retarded and advanced Green's functions of the central disordered region, and $\Gamma_{L,R}$ are the line-width functions coupling left and right terminals to the central region, respectively. In the presence of finite disorder strength, the conductance fluctuation can be obtained by $\mathrm{rms}(G) \equiv \sqrt{\langle G^2\rangle - \langle G\rangle^2}$, where $\langle \ldots \rangle$ represents the ensemble average over different disordered samples at the same strength W. In our calculation, t is set to be the unit of energy E, disorder strength W and spin–orbit coupling strength t_{SO}; and the magnetic field is measured by magnetic flux ϕ/ϕ_0.

3 Fractal structures and density of states

Figure 1(a) displays the system configurations of Sierpinski carpet at different iteration steps. For example, "R_2" indicates the system configuration after the second iteration step [see the middle panel of Fig. 1(a)]. The white parts are set to be empty. Due to the nature of fractal, the structure can be infinitely iterated and the empty regions would become more and more intensive. Figure 1(b) displays density of states as a function of Fermi energy E in the presence of a series of magnetic flux ϕ. For pristine square lattice (i.e., in black line, R_0), Landau level splitting gradually appears along with the increase of magnetic flux ϕ. Meanwhile, the interval of Landau level becomes

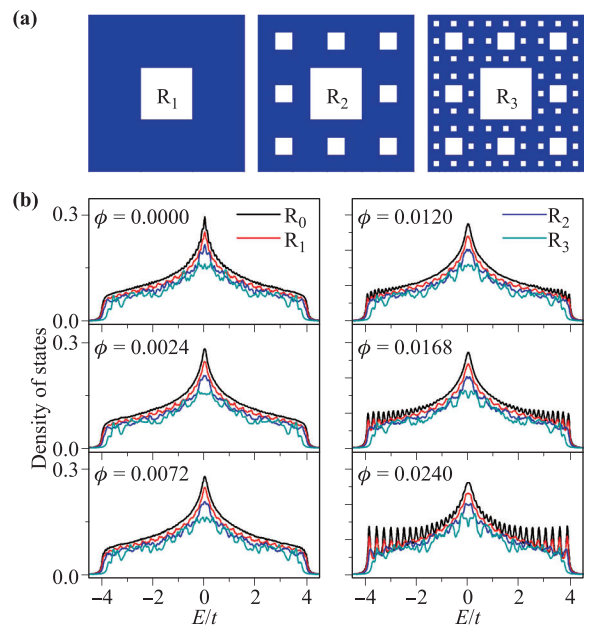

Fig. 1 **(a)** Configurations of the Sierpinski carpet with different iteration steps (e.g., R_2 means two iteration step). The white regions are empty regions. **(b)** Electronic density of states for different iteration steps as a function of Fermi energy E for different magnetic flux ϕ. The system size is set to be $L = 54a$, where a is lattice constant. R_i ($i = 0, 1, 2, \ldots$) indicates different iteration steps, where R_0 is for pristine square lattice and R_i ($i > 0$) is for Sierpinski carpet.

increasing with the increase of ϕ, agreeing well with the theoretical expectations. Compared with that in pristine square lattice system, the density of states of Sierpinski carpet decreases for the whole range of energy. And the more iteration steps of the Sierpinski carpet, the smaller of density of states. At the first iteration step (i.e., the R_1 case where the structure is similar to square lattice except for an empty region in the center), the density of states exhibits the similar characteristic as that of the pristine square lattice. However, one can see that the density of states for structures with larger iteration steps are much more robust against weak magnetic field, implying that stronger magnetic field is required to split their energy levels. This means that the special structure of Sierpinski carpet results in distinct electronic properties. Due to the symmetric feature of density of states about the Fermi energy, we choose a series of E/t within the range of 0 to 4 in our numerical calculation.

4 Conductance fluctuations in systems with different symmetries

4.1 Absence of universal conductance fluctuation in COE symmetry

First, we investigate the average conductance $\langle G\rangle$ and the fluctuation $\mathrm{rms}(G)$ in the Sierpinski carpet with COE

symmetry ($\beta = 1$). Figures 2(a)–(c) display the average conductance as a function of the disorder strength W at different energies by evaluating over 3000 samples at each point. In the absence of disorder, i.e., $W/t = 0$, one can find that $\langle G \rangle$ decays rapidly as the iteration step increases, e.g., at $E/t = 0.2$, the average conductance was decreased to be about 10% from $\sim 63\ e^2/h$ to $\sim 6.3\ e^2/h$ as the iteration step varies from R_1 to R_3. This can be attributed to the strong electron back-scattering from the boundaries of the empty regions. In the presence of disorders (i.e., $W/t > 0$), the average conductance $\langle G \rangle$ decreases along with the increase of the disorder strength. Figures 2(d)–(f) describe the conductance fluctuation rms(G) as a function of disorder strength W. As disorder strength W increases, the conductance fluctuation rms(G) first increases to its maximal plateau, and then gradually decreases. If disorder strength W is strong enough, all electrons in the system would be completely localized to reach the Anderson insulating state, and thus the corresponding conductance fluctuation rms(G) becomes zero. One can find that the peaks of conductance fluctuation that reached its maximum are energy dependent at fixed iteration step, e.g., at R_1 [see Fig. 2(d)], the peak of conductance fluctuation drops from $1.07\ e^2/h$ to $0.93\ e^2/h$ as the Fermi energy increases from $0.2\ t$ to $3.2\ t$. Moreover, the dashed orange line in the figures represents the peak of conductance fluctuation at (R_1, $E/t = 1.4$). From this dashed orange line, we can find that the peak tends to decrease as the iteration step increases, e.g., at $E/t = 1.4$, the peaks corresponding to R_1, R_2, and R_3 are $1.00\ e^2/h$, $0.95\ e^2/h$, and $0.88\ e^2/h$, respectively. From above discussion, we can find that the peaks of conductance fluctuation are dependent on the iteration step and Fermi energy. Therefore, the conductance fluctuation in the COE ($\beta = 1$) symmetry of Sierpinski carpet does not exhibit a universal feature.

4.2 Universal conductance fluctuation in CUE symmetry

Then, we turn to study the conductance fluctuation of CUE system that breaks time-reversal symmetry (i.e., $\beta = 2$). Figures 3(a)–(c) display the average conductance as a function of disorder strength W. In the absence of disorder (i.e., $W/t = 0$), the conductance G at different Fermi energies decreases as iteration step increases. And at fixed magntic flux and Fermi energy, the average conductance also decreases as the disorder strength W increases, similar to that in the COE system. But at the same system parameters, the average conductance in CUE system is smaller than that in COE system due to the enhancement of localized states induced by external magnetic field. At fixed iteration step, e.g., R_1 [see the lines with (ϕ, E) of $(0.012, 1.4)$, $(0.024, 1.4)$, and $(0.048, 1.4)$ in Fig. 3(a)], the average conductance quickly decreases as the magnetic flux increases for weak disorder strength W. When the disorder strength W exceeds certain critical value, such a dependence weakens and results in an saturation of average conductance. Figures 3(d)–(f) display the conductance fluctuation rms(G) as a function of disorder strength W. As illustrated by the dashed orange line, there exists a maximum of rms(G) around $0.78 \pm 0.01(e^2/h)$ for different system configurations, magnetic fluxes, or Fermi energies, suggesting a universal feature of conductance fluctuation [40]. Moreover, the critical

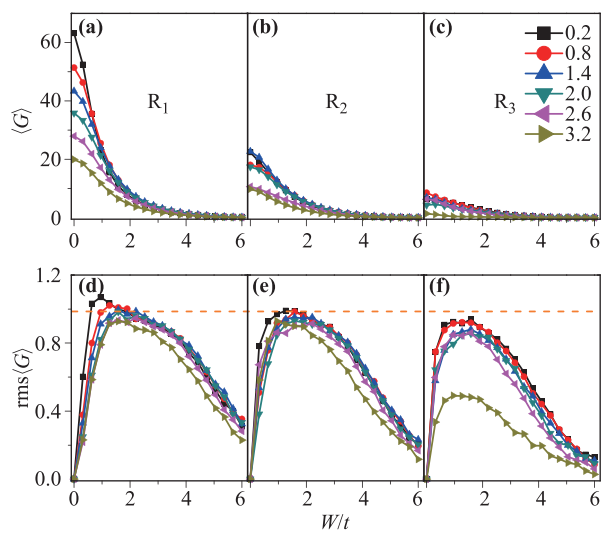

Fig. 2 **(a–c)** Average conductance $\langle G \rangle$ and **(d–f)** its fluctuation rms(G) as a function of disorder strength W at different Fermi energies in the case of $\beta = 1$. The iteration step in the three columns is respective R_1, R_2, and R_3. The system size is $L = 54a$, where a is lattice constant. The Fermi energies are chosen as $E/t = 0.2$, 0.8, 1.4, 2.0, 2.6, and 3.2, respectively. Over 3000 samples are collected for each point.

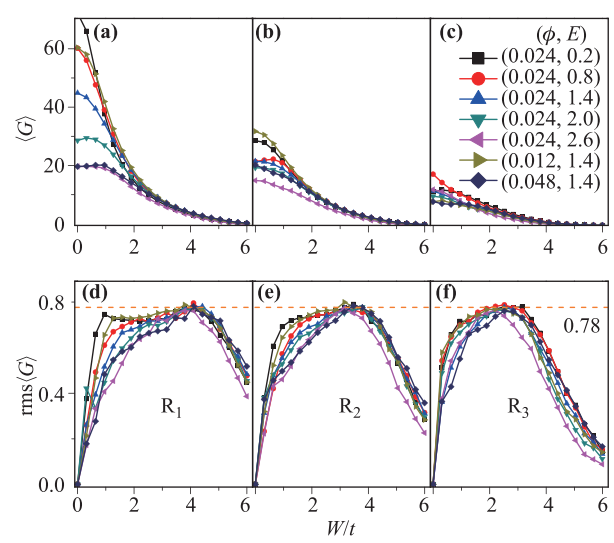

Fig. 3 **(a–c)** Average conductance $\langle G \rangle$ and **(d–f)** its fluctuation as a function of disorder strength W for different magnetic fluxes and energies in the case of $\beta = 2$. The system size is $L = 54a$, where a is lattice constant. Over 3000 samples are collected for each point. The dashed orange line indicates a universal value existing around $0.78 \pm 0.01(e^2/h)$.

disorder strength W_C that reaches the maximum of conductance fluctuation for different Fermi energies exists in a tiny range, and decreases as the iteration step increases, e.g., $W_C/t = 5.26,\ 4.74,\ 3.68$ for R_1, R_2, and R_3, respectively. To confirm it is indeed a universal value, we further study the conductance fluctuation rms(G) for even larger system size. Figure 5(a) displays the maximum of conductance fluctuation in a wide range of system size from $27a$ to $270a$. Due to the finite-size effect, the maximum of conductance fluctuation gradually decreases as the system size increases, and reaches a convergence at larger system size, i.e., the plateau is around $0.74 \pm 0.01(e^2/h)$ when the system size is larger than $162a$. Therefore, different from COE system where the fluctuation does not manifests a universal feature, there exists a universal conductance fluctuation $0.74 \pm 0.01(e^2/h)$ in CUE system with time-reversal symmetry breaking.

4.3 Universal conductance fluctuations in CSE symmetry

Next, we move to explore the conductance fluctuation of systems with CSE symmetry (i.e., $\beta = 4$). Figures 4(a)–(c) display the average conductance as a function of disorder strength W. One can find some universal features of the variation of average conductance in COE, CUE, and CSE systems, i.e., the average conductance decreases with the increase of iteration steps, Fermi energies, or disorder strength. Moreover, the average conductance increases as the spin–orbit coupling strength increases [see the curves with (t_{SO}, E) of $(0.2, 1.7)$, $(0.4, 1.7)$, and $(0.6, 1.7)$ in Figs. 4(b) or (c)]. Figures 4(d)–(f) display the conductance fluctuation rms(G) as a function of disorder strength W. The dashed orange line in these figures denotes the maximum of rms(G) around $0.75 \pm 0.01(e^2/h)$ at different iteration steps, spin–orbit coupling strengths, and Fermi energies. All these together indicate the presence of universal conductance fluctuation in the CSE system. In addition, the critical disorder strength W_C at fixed t_{SO} decreases as the iteration step increases (e.g., in the case of $t_{SO} = 0.4$ and $E/t = 1.2$, $W_C \approx 5.26$, 4.74, and 3.68 for R_1, R_2, and R_3 respectively). By further investigating the maxima of conductance fluctuation in a wide range of system size from $27a$ to $162a$ [see Fig. 5(b)], one can find that the system size shows little influence on the conductance fluctuation plateau, which is around $0.74 \pm 0.01(e^2/h)$. Therefore, we conclude that there also exists a universal conductance fluctuation in systems with CSE symmetry. In addition, the difference of the size effect of UCF in CUE and CSE indicates that time-reversal symmetry has significant influence on electronic transport in a disordered system with different size. A phenomenological picture of band structure can be used to explain the difference. In a magnetic field, electronic band will form Landau level and this is a *global* influence on the band structure. The number of Landau levels depend on the strength of magnetic field, as well as system size. On the contrary, bands structure will open band gaps at the crossing points when Rahsba spin–orbit coupling is considered and the system size have little influence on the electronic band structure. This is a *local* influence on the band structure. Therefore, UCF in CUE decrease gradually to a saturation as the increase of system size; while it seems unchanged in CSE.

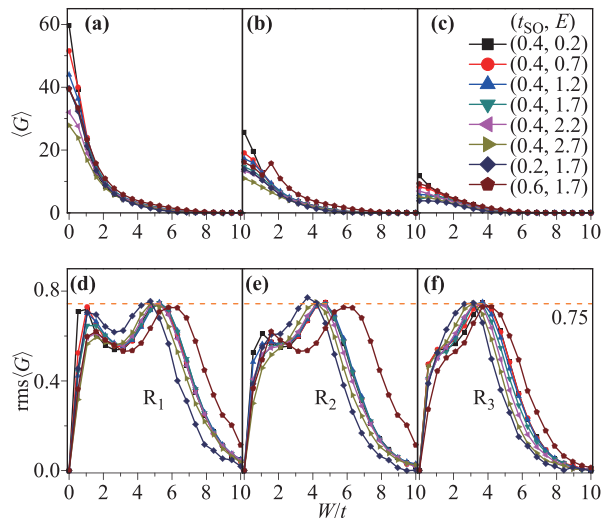

Fig. 4 **(a–c)** Average conductance $\langle G \rangle$ and **(d–f)** its fluctuation as a function of disorder strength W for different t_{SO} and energies in the case of $\beta = 4$. The system size is $L = 54a$, where a is lattice constant. Over 3000 samples are collected for each point. The dashed orange line indicates a universal value around $0.75 \pm 0.01(e^2/h)$.

5 Conductance distributions in both CUE and CSE

From above discussions, one can reach that the Sierpinski carpet does not exhibit a universal feature of conduc-

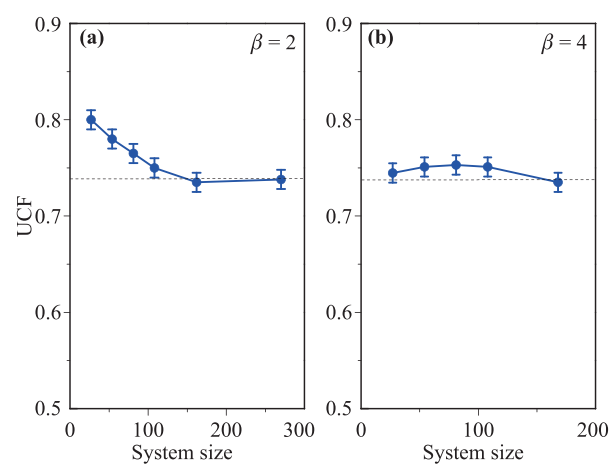

Fig. 5 The size effect of UCF in the case of **(a)** $\beta = 2$ and **(b)** $\beta = 4$. The data is collected from the size of $27a$, $54a$, $81a$, $108a$, $162a$ and $270a$. The curve shows a convergence behavior.

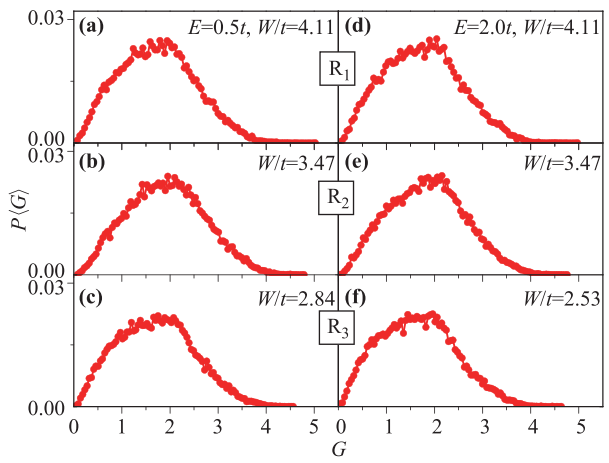

Fig. 6 Conductance distribution at the critical disorder strength W_C in CUE system ($\beta = 2$) for $\phi/\phi_0 = 0.012$. The Fermi energies in **(a–c)** and **(d–f)** are $E/t = 0.5$ and $E/t = 2.0$, respectively. The first, second and third rows represent R_1, R_2, and R_3, respectively. The system size is $L = 54a$, where a is lattice constant. Over 30000 samples are collected.

tance fluctuations in COE system, but reaches a universal conductance fluctuation of $0.74 \pm 0.01(e^2/h)$ for both CUE (time-reversal symmetry breaking) and CSE (spin-rotation symmetry breaking) symmetries. To further reveal the physical mechanism of the universal conductance fluctuations in Sierpinski carpet, we study the conductance distribution around the critical disorder strength W_C. Figure 6 displays the conductance distribution $P(G)$ near the critical disorder strength W_C in CUE system ($\beta = 2$). One can find that the general function of the conductance distribution is independent of Fermi energies or iteration steps, i.e., the left regime obeys the Gaussian distribution function, while the right regime obeys the log-normal distribution function. In the CSE systems, we also find that the conductance near the critical disorder strength follows the same distribution function as that in the case of CUE symmetry (see Fig. 7). Therefore, one can conclude that in the Sierpinski carpet, both CUE and CSE systems share the same universal conductance fluctuations and conductance distribution near the critical disorder strength.

As displayed in Fig. 8, we further study the conductance distribution beyond the critical disorder strength W_C. In CUE system [see Figs. 8(a)–(c)], the conductance distribution belongs to Gaussian function when disorder strength W less than W_C [see Fig. 8(a)], indicating the system stays in the ballistic regime. While it follows the log-normal distribution when disorder strength W is larger than W_C [see Fig. 8(c)], implying that the system enters the localized regime [7, 14]. In particular, the conductance distribution experiences a transition from Gaussian to log-normal function around W_C as mentioned above. In CSE system [see Figs. 8(d)–(f)], the variation of conductance distribution around the critical disorder strength W_C behaves similar as that in CUE system. Therefore, from the analysis of conductance distribution, we can conclude that the universal conductance fluctuation in Sierpinski carpet occurs in the crossover region between ballistic and Anderson localization regime in both CUE and CSE systems.

6 Summary

In this work, we theoretically investigate the electronic transport properties (e.g., conductance and its fluctuation) of disordered two-terminal device in Sierpinski carpet for circular orthogonal, circular unitary, and circular symplectic ensembles. Our results show that there exist universal conductance fluctuations in both CUE and CSE

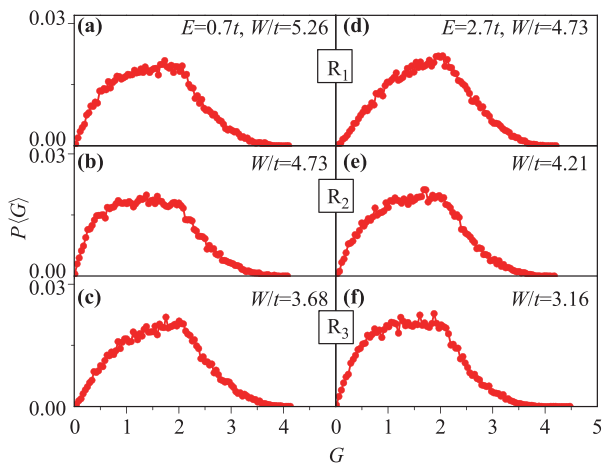

Fig. 7 Conductance distribution around the critical disorder strength in the case of $\beta = 4$ for $t_{SO} = 0.4t$. The Fermi energies in **(a–c)** and **(d–f)** are $E/t = 0.7$ and $E/t = 2.7$, respectively. The first, second and third rows represent R_1, R_2, and R_3, respectively. The system size is $L = 54a$, where a is lattice constant. Over 30000 samples are collected for each point.

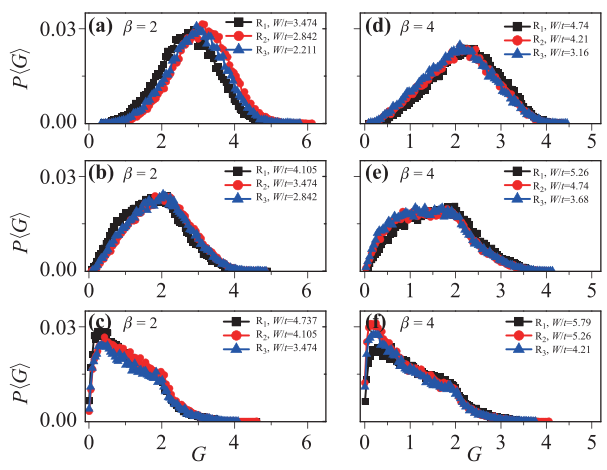

Fig. 8 Variation of conductance distribution in different disorder strengths W. **(a)** and **(d)** is for $W < W_C$. **(b)** and **(e)** is for $W = W_C$. **(c)** and **(f)** for $W > W_C$. (a)–(c) correspond to $\beta = 2$. (d)–(f) correspond to $\beta = 4$.

systems, while not in the COE system [41]. By further studying the conductance distribution around the critical disorder strength W_C in CUE and CSE systems, we find that both of systems share the same distribution function, which obeys Gaussian distribution when $W < W_C$ or follows log-normal distribution when $W > W_C$, indicating that the universal conductance fluctuations in both CUE and CSE systems occur in the crossover region between ballistic and Anderson localized regimes. In integer dimensions, the universal conductance fluctuations in metal-insulator crossover regime have been studied by Qiao *et al.* [14]. Compared to aforementioned study, universal conductance fluctuations in Sierpinski carpet have different values, indicating the difference between the universal conductance fluctuations in fractal and integer dimensions. Our finding in Sierpinski carpet can be extended to study other fractal structures that have different Hausdorff dimensions.

Acknowledgements This work was financially supported by the National Key Research and Development Program (Grant Nos. 2017YFB0405703 and 2016YFA0301700), the National Natural Science Foundation of China (Grant No. 11474265), and Anhui Initiative in Quantum Information Technologies. We thank the supercomputing service of AM-HPC and the Supercomputing Center of USTC for providing the high-performance computing resources.

References and notes

1. W. Ji, H. Q. Xu, and H. Guo, Quantum description of transport phenomena: Recent progress, *Front. Phys.* 9(6), 671 (2014)
2. J. Zhuang, Y. Wang, Y. Zhou, J. Wang, and H. Guo, Impurity-limited quantum transport variability in magnetic tunnel junctions, *Front. Phys.* 12(4), 127304 (2017)
3. H. Z. Lu and S. Q. Shen, Quantum transport in topological semimetals under magnetic fields, *Front. Phys.* 12(3), 127201 (2017)
4. L. B. Altshuler, Fluctuations in the extrinsic conductivity of disordered conductors, *JETP Lett.* 41, 648 (1985)
5. P. A. Lee and A. D. Stone, Universal conductance fluctuations in metals, *Phys. Rev. Lett.* 55(15), 1622 (1985)
6. P. A. Lee, A. D. Stone, and H. Fukuyama, Universal conductance fluctuations in metals: Effects of finite temperature, interactions, and magnetic field, *Phys. Rev. B* 35(3), 1039 (1987)
7. C. W. J. Beenakker, Random-matrix theory of quantum transport, *Rev. Mod. Phys.* 69(3), 731 (1997)
8. S. B. Kaplan and A. Hartstein, Universal conductance fluctuations in narrow Si accumulation layers, *Phys. Rev. Lett.* 56(22), 2403 (1986)
9. A. García-Martín and J. J. Sáenz, Universal conductance distributions in the crossover between diffusive and localization regimes, *Phys. Rev. Lett.* 87(11), 116603 (2001)
10. W. Ren, Z. Qiao, J. Wang, Q. Sun, and H. Guo, Universal spin-Hall conductance fluctuations in two dimensions, *Phys. Rev. Lett.* 97(6), 066603 (2006)
11. Z. Qiao, J. Wang, Y. Wei, and H. Guo, Universal quantized spin-Hall conductance fluctuation in graphene, *Phys. Rev. Lett.* 101(1), 016804 (2008)
12. M. Yu. Kharitonov and K. B. Efetov, Universal conductance fluctuations in graphene, *Phys. Rev. B* 78(3), 033404 (2008)
13. J. Wurm, A. Rycerz, I. Adagideli, M. Wimmer, K. Richter, and H. U. Baranger, Symmetry classes in graphene quantum dots: Universal spectral statistics, weak localization, and conductance fluctuations, *Phys. Rev. Lett.* 102(5), 056806 (2009)
14. Z. Qiao, Y. Xing, and J. Wang, Universal conductance fluctuation of mesoscopic systems in the metal-insulator crossover regime, *Phys. Rev. B* 81(8), 085114 (2010)
15. Z. M. Liao, B. H. Han, H. Z. Zhang, Y. B. Zhou, Q. Zhao, and D. P. Yu, Current regulation of universal conductance fluctuations in bilayer graphene, *New J. Phys.* 12(8), 083016 (2010)
16. Z. Qiao, W. Ren, and J. Wang, Universal spin-Hall conductance fluctuations in two-dimensional mesoscopic systems, *Mod. Phys. Lett. B* 25(06), 359 (2011)
17. Z. Li, T. Chen, H. Pan, F. Song, B. Wang, J. Han, Y. Qin, X. Wang, R. Zhang, J. Wan, D. Xing, and G. Wang, Two-dimensional universal conductance fluctuations and the electron-phonon interaction of surface states in Bi_2Te_2Se microflakes, *Sci. Rep.* 2(1), 595 (2012)
18. E. Rossi, J. H. Bardarson, M. S. Fuhrer, and S. Das Sarma, Universal conductance fluctuations in Dirac materials in the presence of long-range disorder, *Phys. Rev. Lett.* 109(9), 096801 (2012)
19. Z.-G. Li, S. Zhang, and F.-Q. Song, Universal conductance fluctuations of topological insulators, *Acta Physica Sinica* 64(8), 97202 (2015)
20. L.-X. Wang, S. Wang, J.-G. Li, C.-Z. Li, D. P. Yu, and Z.-M. Liao, Universal conductance fluctuations in Dirac semimetal Cd_3As_2 nanowires, *Phys. Rev. B* 94, 161402(R) (2016)
21. Y. Hu, H. Liu, H. Jiang, and X. C. Xie, Numerical study of universal conductance fluctuations in three-dimensional topological semimetals, *Phys. Rev. B* 96(13), 134201 (2017)
22. Y. Q. Li, K. H. Wu, J. R. Shi, and X. C. Xie, Electron transport properties of three-dimensional topological insulators, *Front. Phys.* 7(2), 165 (2012)
23. B. B. Mandelbrot, How long is the coast of Britain? Statistical self-similarity and fractional dimension, *Science* 156(3775), 636 (1967)
24. B. B. Mandelbrot, Self-affine fractals and fractal dimension, *Phys. Scr.* 32(4), 257 (1985)
25. R. Rammal, Nature of eigenstates on fractal structures, *Phys. Rev. B* 28(8), 4871 (1983)
26. A. Chakrabarti and B. Bhattacharyya, Sierpinski gasket in a magnetic field: Electron states and transmission characteristics, *Phys. Rev. B* 56(21), 13768 (1997)

27. X. R. Wang, Localization in fractal spaces: Exact results on the Sierpinski gasket, *Phys. Rev. B* 51(14), 9310 (1995)
28. Y. Asada, K. Slevin, and T. Ohtsuki, Possible Anderson transition below two dimensions in disordered systems of noninteracting electrons, *Phys. Rev. B* 73(4), 041102 (2006)
29. M. K. Schwalm and W. A. Schwalm, Length scaling of conductance distribution for random fractal lattices, *Phys. Rev. B* 54(21), 15086 (1996)
30. Y. Liu, Z. Hou, P. M. Hui, and W. Sritrakool, Electronic transport properties of Sierpinski lattices, *Phys. Rev. B* 60(19), 13444 (1999)
31. Z. Lin, Y. Cao, Y. Liu, and P. M. Hui, Electronic transport properties of Sierpinski lattices in a magnetic field, *Phys. Rev. B* 66(4), 045311 (2002)
32. C. Y. Ho and C. R. Chang, Spin transport in fractal conductors with the Rashba spin–orbit coupling, *Spin* 02(02), 1250008 (2012)
33. B. R. Lee, C. R. Chang, and I. Klik, Spin transport in multiply connected fractal conductors, *Spin* 04(03), 1450007 (2014)
34. E. van Veen, S. Yuan, M. I. Katsnelson, M. Polini, and A. Tomadin, Quantum transport in Sierpinski carpets, *Phys. Rev. B* 93(11), 115428 (2016)
35. M. Brzezińska, A. M. Cook, and T. Neupert, Topology in the Sierpiński–Hofstadter problem, *Phys. Rev. B* 98(20), 205116 (2018)
36. J. Shang, Y. Wang, M. Chen, J. Dai, X. Zhou, J. Kuttner, G. Hilt, X. Shao, J. M. Gottfried, and K. Wu, Assembling molecular Sierpiński triangle fractals, *Nat. Chem.* 7(5), 389 (2015)
37. S. N. Kempkes, M. R. Slot, S. E. Freeney, S. J. M. Zevenhuizen, D. Vanmaekelbergh, I. Swart, and C. M. Smith, Design and characterization of electrons in a fractal geometry, *Nat. Phys.* 15(2), 127 (2019)
38. Z. Qiao, W. Ren, J. Wang, and H. Guo, Low-field phase diagram of the spin Hall effect in the mesoscopic regime, *Phys. Rev. Lett.* 98(19), 196402 (2007)
39. S. Datta, Electronic Transport in Mesoscopic Systems, Cambridge: Cambridge University Press, England, 1995
40. It should be noted that the rms(G) in Figs. 3 and 4 seem not to be exactly same mainly due to discrete distribution of disorder strength W in numerical method. In order to reasonably describe the universal conductance fluctuations, we use a range of $[-0.1, 0.1]$ (e^2/h) based on the UCF value. The same method also used in other papers (Refs. [10–12]).
41. In circular orthogonal ensemble, there does not exist a metal-insulator transition when system dimension below 3 according to the scaling theory of localization. Therefore, there is not UCF in circular orthogonal ensemble.